Three-dimensional reconstruction by computed tomography of an undifferentiated sarcoma in a dog

Rafael Zafra , Conrado Carrascosa , Alejandro Suarez-Bonnet , Carlos Melián , Teresa Fernández , Miguel Monzón , Oscar Quesada , Francisco Suarez & J. Raduan Jaber

Three-dimensional reconstruction by computed tomography of an undifferentiated sarcoma in a dog

Rafael Zafra, Conrado Carrascosa, Alejandro Suarez-Bonnet, Carlos Melián, Teresa Fernández, Miguel Monzón, Oscar Quesada, Francisco Suarez and J. Raduan Jaber*

Department of Morphology, Faculty of Veterinary Medicine, University Las Palmas de Gran Canaria. Las Palmas de Gran Canaria, Spain

The purpose of this paper was to show a three-dimensional computed tomographic reconstruction of the undifferentiated sarcoma in a dog. Two-millimetre-thick transverse images were obtained. Images provided excellent anatomic detail of the severity of the tumour and can be a valuable diagnostic aid for clinical evaluation of several types of neoplasias in dogs. Computed tomography provides detailed information regarding the extent of disease and accurate discrimination of neoplastic versus non-neoplastic diseases. In addition, this technique can be used as a tool for teaching clinical anatomy in veterinary schools.

Keywords: 3D reconstruction; computed tomography; neoplasia; anatomy; dog

Introduction

Cancer in companion animals is a leading cause of death. The prevalence of these diseases is increasing and a number of factors are contributing to this increase, in part reflecting the ageing of our canine and feline population. It is the most common cause of orbital mass in the dog. Orbital diseases in general are not as common in cats. In both dogs and cats more than 90% of orbital tumours are malignant. Osteosarcoma, fibrosarcoma and nasal adenocarcinoma have been the most common tumour types (Hendrix and Gelatt 2000), although other types of tumours such as soft tissue or spindle cell sarcomas have been also identified (North and Banks 2009).

A computed tomography (CT) or magnetic resonance imaging scans are the imaging tools of choice in all cases where an orbital and retrobulbar tumours are suspected. CT also allows better evaluation of bony lesions, including the extent of bone tumours and the involvement of bone in soft tissue tumours adjacent to bone (Rogers et al. 1996; North and Banks 2009). The recent advances and refinements in CT technology involve the application of computer software for the generation of three-dimensional (3D) reconstruction of an area of anatomic interest (Grossman 1990). This technique requires multiple thin section images and advantages of this procedure are that anatomical detail is improved and bony structures can be imaged with different degrees of rotation (Kraus et al. 1997). CT reconstruction has been applied previously to study the anatomy of the immature California sea lion head (Dennison and Schwarz 2008) or the normal equine cervical spine in two neonatal foals (Zafra et al. 2011). In relation to clinical diseases, this technique has been used for assessment of canine cervical and lumbar spine (Drees et al. 2009a) and the extension of neoplastic and non-neoplastic processes (Saunders et al. 2003). Most of the tumoural processes evaluated by 3D reconstruction have been diagnosed as squamous cell carcinoma of the canine nasal cavity and frontal sinus (Roger et al. 1996). However, to date there are not descriptions of other types of tumours affecting to different areas of the skull. The purpose of this short communication was to report a 3D reconstruction by computer tomography of an undifferentiated sarcoma in a dog.

Material and methods

An 11-year-old male mixed breed dog arrived to the Veterinary Hospital of the University of Las Palmas de Gran Canaria, Canary Islands, Spain. In the physical examination, the animal showed a mass formation located at the orbital region. The dog presented neurological signs due to direct invasion of the cranial vault by tumour. A bone biopsy punch was used to biopsy this bony lesion. Formalin-fixed tissues were routinely processed, embedded in paraffin, sectioned at 5 μm, and stained with haematoxylin and eosin for histological examination.

The CT images were obtained after sedation with xylazine at 0.5 mg/kg, IV (Rompun®, Bayer

---

HealthCare AG, Germany). The anaesthesia was induced with a bolus of propofol at 2.0–2.5 mg/kg, IV (Diprivan®, AstraZeneca, UK) administered through a jugular catheter. The dog was intubated with a cuffed endotracheal tube to maintain an airway and placed in sternal recumbence on the scanning table. The animal was monitored by counting respiratory and pulse rates. A series of 2-mm thick transverse images from the head to the second cervical verterbra was obtained using a fourth-generation CT equipment (General Electric Medical System, Milwaukee, WI). The parameters used for CT imaging were 120 kVp, 560 mAs. To better evaluate the extension of the tumoral process, a 3D reconstruction was performed with special emphasis on the orbital region, as well as the frontal and parietal bones.

Results

Histologically, the biopsy tissue consisted of a neoplastic proliferation of anaplastic and pleomorphic cells with a fusiform to epithelioid shape with moderate eosinophilic cytoplasm (Figure 1). These cells had large round to oval nuclei and conspicuous nucleoli. Mitoses figures were abundant ($>3/10$ high-powered field (HPF)) with occasional bizarre appearance. These plump spindle cells arranged in a haphazard pattern of growth with areas of cells oriented in interwoven bundles and in a whorled way. Given the high grade of atipia, lack of differentiation and anaplastic features, identification of the cell of origin could not be determined.

Undifferentiated sarcoma observed in the dog of the present study was evaluated by CT and it showed a characteristic rounded, well-defined lesion with
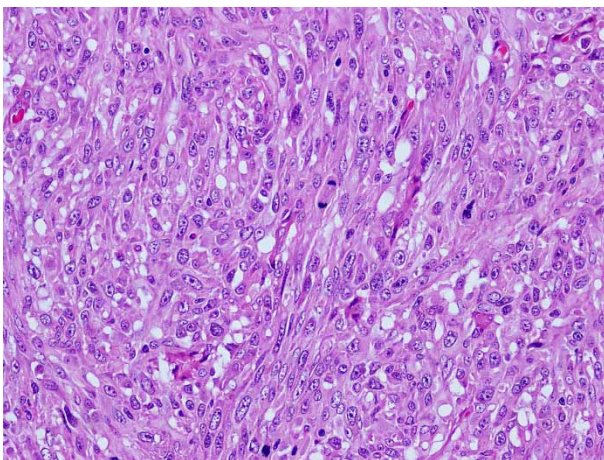

Figure 1. Skull, undifferentiated sarcoma of a dog showing proliferation of anaplastic and pleomorphic cells with a fusiform to epithelioid shape with moderate eosinophilic cytoplasm. H&E × 40.

non-homogeneous bone opacity. A 3D reconstruction was done to analyse the extent of the bony lesions produced by this tumour. Several images with excellent anatomic details were obtained but only the most representatives were selected. Thus, the first image shows a lateral reconstruction of the head where a mass formation can be visualised. This mass was occupying the entire orbital region, extended from the lateral part of the face, affecting the antero-inferior or maxillary border of the zygomatic bone ventrally, whereas more dorsally it was prolonged upward to the frontal bone (Figure 2a). In the second 3D image, extraorbital involvement was detected. This image was focused on frontal and parietal areas, where bone lysis and invasion into the cranial cavity were noted (Figure 2b). Thus, the upper boundary of the base of the orbit also called the supraorbital margin was affected as can be seen in the image (Figure 2b), where neoformation of bone tissue was also seen. Bone destruction was noted at the roof of the cranium, including the frontal and the parietal bones and up to the interparietal bones.

Discussion

Osteosarcoma, fibrosarcoma and nasal adenocarcinoma have been the most common tumour types diagnosed in this area in dogs. These types of tumours are more common in purebred, female and middle-aged dogs, where most tumours are primaries (North and Banks 2009). In our case, the tumoral process was identified in a mixed, old male dog and it was diagnosed as undifferentiated sarcoma that to date had not been evaluated by CT.

Recently, the availability of used equipment and tolerable service cost has allowed a low, but steady, increase in the use of CT imaging in veterinary medicine (Barbee et al. 1987; Allen et al. 1988; Feeney et al. 1991; Drees et al. 2009a). CT with 3D reconstruction has been a valuable diagnostic aid for clinical evaluation of cervical vertebral malformations, degeneratives changes of articular facets or cervical static stenosis in domestic animals (Drees et al. 2009a). There are different studies that indicate a high accuracy of CT for diagnosis of dogs with head tumours (Saunders et al. 2003; Dress et al. 2009b). We have attempted to describe our observations on recognisable anatomic structures that can be used as a tool to establish the tumour extension, but further studies are necessary to define the ultimate limits of 3D CT reconstruction both for basic morphologic imaging and for interpretation of patient images with clinical signs. Much of this will, however, have to come from continued clinical experience and the ongoing comparison
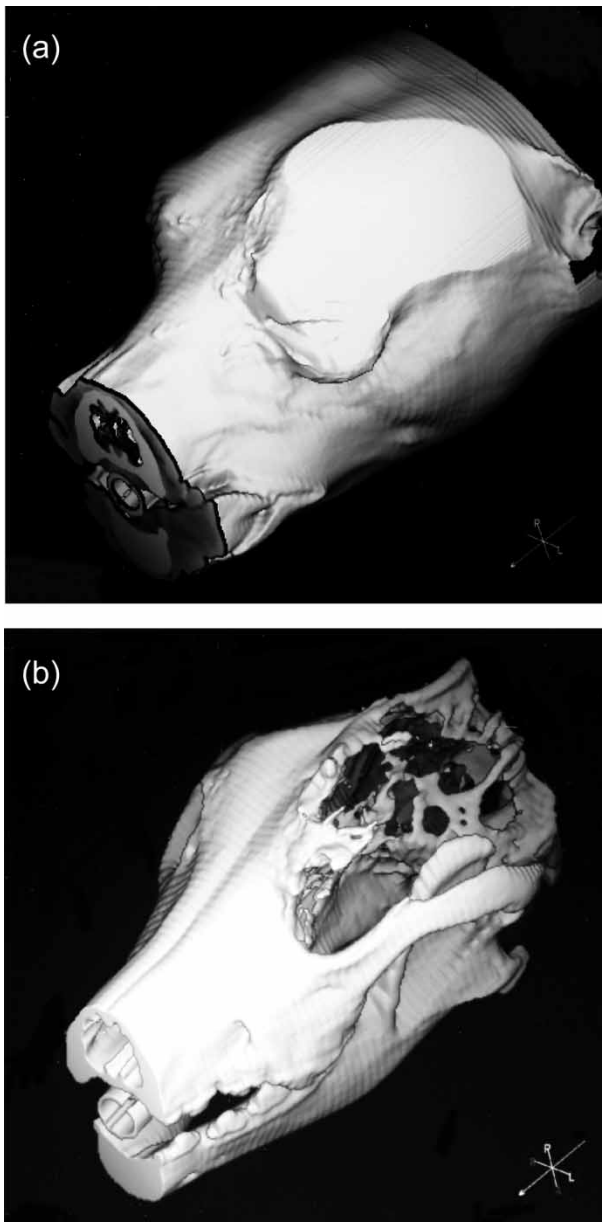
Figure 2. Three-dimensional reconstructed CT image of the skull. (a) Lateral reconstruction of the head where a mass formation occupying the orbital fossa is visualised. (b) 3D image with extraorbital involvement and focused on frontal and parietal areas, showing bone lysis and invasion into the cranial cavity.

between imaged anatomy or pathology and case outcome or post-mortem studies.

In conclusion, CT 3D images are especially useful for surgical planning, particularly if an aggressive resection with curative intent is planned. On the teaching front, 3D imaging technology may facilitate teaching of anatomy to veterinary students by allowing the view of structures in a realistic, 3D manner. Thus, this technique is an anatomical tool that enables visualisation of bone, vascular network and selected soft tissue anatomy in a 3D image. This procedure eliminates the difficulties of visualising the extension of the process and facilitates to see the invasive capacity of different types of neoplasias.

References

Allen J, Barbee D, Crisman M. 1988. Diagnosis of equine pituitary tumors by computed tomography. Part 1. Compendium Equine 10:1103–1105.

Barbee D, Allen J, Gavin P. 1987. Computed tomography in horses. Technique. Veterinary Radiology 28:144–151.

Dennison SE, Schwarz T. 2008. Computed tomographic imaging of the normal immature California sea lion head (*Zalophus californianus*). Veterinary Radiology & Ultrasound 49:557–563.

Drees R, Dennison SE, Keuler NS, Schwarz T. 2009a. Computed tomographic imaging protocol for the canine cervical and lumbar spine. Veterinary Radiology & Ultrasound 50:74–79.

Drees R, Forrest LJ, Chappell R. 2009b. Comparison of computed tomography and magnetic resonance imaging for the evaluation of canine intranasal neoplasia. Journal of Small Animal Practice 50:334–340.

Feeney DA, Fletcher TF, Hardy RM. 1991. Atlas of correlative imaging anatomy of the normal dog: ultrasound and computer tomography. Philadelphia: W.B. Saunders.

Grossman C. 1990. Magnetic resonance imaging and computed tomography of the head and spine. Baltimore: Williams & Wilkins.

Hendrix DV, Gelatt KN. 2000. Diagnosis, treatment and outcome of orbital neoplasia in dogs: a retrospective study of 44 cases. Journal of Small Animal Practice 41:105–108.

Kraus M, Mahaffey M, Girard E, Chambers J, Brown C, Coates J. 1997. Diagnosis of C5-C6 spinal luxation using three-dimensional computed tomographic reconstruction. Veterinary Radiology & Ultrasound 38:39–41.

North S, Banks T. 2009. Small animal oncology: an introduction. London: Saunders.

Rogers KS, Walker MA, Helman RG. 1996. Squamous cell carcinoma of the canine nasal cavity and frontal sinus: eight cases. Journal of American Animal Hospital Association 32:103–110.

Saunders JH, van Bree H, Gielen I, de Rooster H. 2003. Diagnostic value of computed tomography with chronic nasal disease. Veterinary Radiology & Ultrasound 44:409–413.

Zafra R, Carrascosa C, Rivero M, Peña S, Fernández T, Suarez-Bonnet A, Jaber JR. 2011. Analysis of equine cervical spine using 3D computed tomographic reconstruction. Journal of Applied Animal Research (in press).